Eur. Radiol. 12 (Suppl. 2) S17-S24 (2002)

Multidetector-row CT cardiac imaging with 4 and 16 slices for coronary CTA and imaging of atherosclerotic plaques

Andreas F. Kopp[1], Axel Küttner[1], Martin Heuschmid[1], Stephen Schröder[2], B. Ohnesorge[3], C.D. Claussen[1]

[1] Department of Diagnostic Radiology, [2]Department of Internal Medicine, Division of Cardiology, Eberhard-Karls-University, Tuebingen, Germany, [3]Siemens Medical Systems, Forchheim, Germany

Introduction

Despite a multitude of different medical and interventional strategies to treat coronary artery disease (CAD), the natural course of CAD is a relentless progression. The current gold standard to assess the degree of stenosis is coronary angiography. In Germany alone, the total number of angiographic procedures rose by 45% from 1995 to 2000, while the fraction of interventional procedures remained almost constantly low at about 30% [1]. Although coronary angiography has become a safe procedure with only a small risk associated [2], the inconvenience for the patient as well as the economic burden have fueled the quest to find an alternative, noninvasive method to visualize and assess coronary arteries. In the last two years mechanical multidetector-row CT (MDCT) systems with simultaneous acquisition of four slices and half-second scanner rotation have become available [3-5]. Multi-row acquisition with these scanners allows for considerably improved visualization of the coronary arteries [6]. Initial experiences have shown that coronary lesions can be detected with good sensitivity and specificity [5, 7-10].

Data acquisition with MDCT

Cardiac MDCT imaging can be done using two basic modes of operation for image acquisition: prospective triggering and retrospective gating [11]. *Retrospective gating* is needed for spiral scanning. Retrospective electrocardiography (ECG)-gating was observed to improve cardiac image quality compared to prospective ECG-triggering techniques due to overlapping image reconstruction and reduced sensitivity to cardiac arrhythmia [12, 13].

Calcium scoring

Current electron beam CT protocols are used for measuring coronary arterial calcification by acquiring a stack of contiguous 3-mm sections [14]. The calcium score, as originally proposed by Agatston [15], is determined on the basis of the product of the total area of a calcified plaque and an arbitrary scoring system for those pixels with an attenuation greater than 130 HU. Theoretically, this multisection data set should give a clear representation of the amount of calcification in the major coronary arterial tree, yet high interscan variability up to 60% has impaired the ability to measure coronary arterial calcification precisely and repeatedly [16]. Spiral multislice CT holds promise to overcome this limitation: coupling the technique of retrospective gating with nearly isotropic volumetric imaging significantly improved the reliability of coronary calcium quantification, especially for small plaques [17]. Using ECG-gated volume coverage with multislice spiral CT and overlapping image reconstruction (2.5 mm collimation, 1 mm increment), an interscan variability of approximately 5%-8% can be achieved [18]. With the advent of multislice CT with significantly reduced interstudy variability, we can now begin to define the effects of treatment regimens on coronary arterial calcification and to determine whether changes in coronary arterial calcification in individual patients have predictive value for future coronary events. If these differences in calcium score over time result in a difference in event rates, it is conceivable that serial measurements of calcium score by MDCT will provide a powerful and much needed predictive tool [19].

Coronary CTA for detection of stenoses

The imaging protocol for MDCT angiography of the coronary arteries is relatively straightforward. To establish the scan delay time, a test bolus of 15 ml contrast medium (CM) and a chaser bolus of 20 ml saline are used. The circulation time is determined by measuring CT density values in the ascending aorta. Imag-

ing commences at the circulation time plus 3 s [20]. A bolus of 120 ml nonionic contrast (400 mg/ml iodine) is injected through an 18-gauge catheter into an antecubital vein [21]. The concentration of 400 mg I/ml was selected for the imaging protocol, because it is important to achieve a high concentration rapidly. Higher attenuation values are thus achieved in the arteries with the same amount of contrast medium as compared to the standard iodine concentration (300 mg I/ml). This permits depiction of smaller vessels, facilitates postprocessing and reduces the overall volume of contrast medium required by approximately 30% (Tables 1, 2). The angiographic series is a continuous spiral scan with the calculated pitch. The z-resolution is significantly improved compared to electron beam CTA, where only sequential ECG-triggered 3-mm slices can be obtained. With MDCT technology, 1-mm slices and submillimeter image increment provide a three-dimensional (3D) data set within a single breath-hold for high resolution CT volume imaging [22]. For optimal image quality, the reconstruction window within the cardiac cycle should be selected individually for each of the three major coronary arteries [13, 23, 24]. Data from CT angiography are transferred to a computer workstation for post-processing (Figs. 1, 2).

Even with 4-row technology, noninvasive MDCTA showed a high diagnostic accuracy in the detection and quantification of coronary lesions [25]. The results of coronary MDCT angiography obtained so far from different centers are encouraging: CTA of the coronary arteries has a sensitivity of 40%-91%, a specificity of 71%-97%, a positive predictive value of 0.7-0.9, and a negative predictive value of 0.8-0.9 for detection of hemodynamically significant stenoses in the major segments of the coronary arteries (Table 3) [26]. Not only severe, but also intermediate lesions were visualized [26]. Furthermore, MDCT angiography yielded promising results for assessment of bypass graft patency [5].

Table 1. Protocol MDCTA coronary arteries

- Precontrast scan (low dose, collimation 4 x 2.5 mm)
- Circulation time: 20 cc CM (400 mg/cc), 20 cc NaCl
- CT density in ascending aorta over 20 s following 10 s pi, every 2 s
- Antecubital vein
- Iomeron 400 (400 mgl/cc)
- Biphasic injection: 50 cc @ 4 cc/s, then 2.5 cc/s
- Volume: 120-140 cc

Table 2. High concentration contrast agents

- High concentration of iodine must be rapidly reached
- Increase of attenuation values in the arteries with the same amount of iodine compared to standard iodine concentration (300 mgl/ml)
- Depiction of smaller vessels
- Facilitates postprocessing
- Reduction of the overall amount of c.m. of approx 30%

Table 3. Sensitivity and specificity of MDCT angiography (MDCTA) in the detection of hemodynamically relevant stenoses

References	Patients n	Sensitivity %	Specificity %
Kopp et al. [47]	102	86	93
Achenbach et al. [48]	64	91	84
Becker et al. [7]	48	82	97
Nieman et al. [10]	31	91	97
Nitatori et al. [49]	18	40	71
Fischbach et al. [50]	27	76	93
Herzog et al. [51]	120	71	92

a **b** **c** **d**

Fig. 1a-d. *MDCT angiography.* Imaging parameters were: collimation 4×1 mm, pitch 1.5, 120 cc Iomeprol 400. **a** Anterior view of left coronary artery with left anterior descending (LAD) in volume rendering technique. **b** Lateral view of left coronary artery with LAD and circumflex branch. **c** Maximum intensity projection of right coronary artery (RCA) with calcified plaques (*arrow*). **d** Diaphragmatic surface with posterolateral and interventricular branches of RCA (*arrows*)

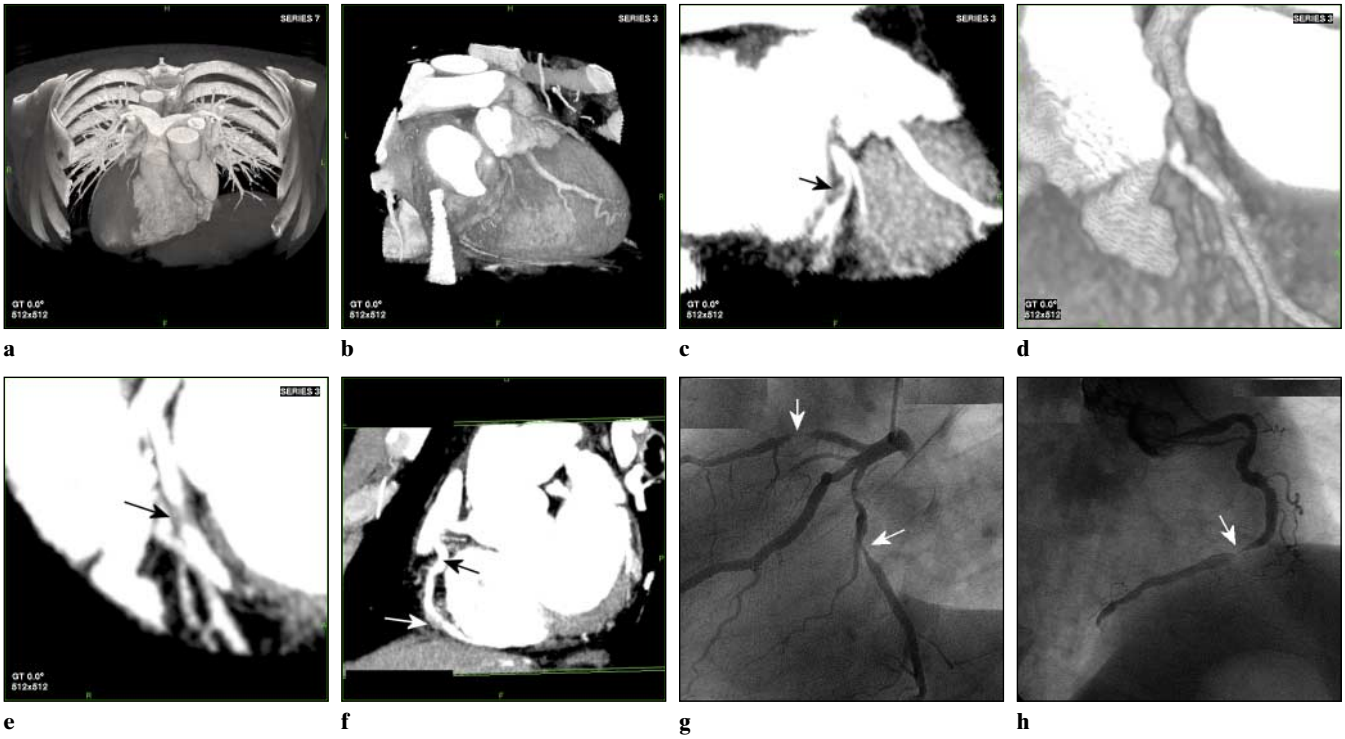

Fig. 2a-h. *Male patient, age 55 years, with "situs inversus" and 2-vessel-disease.* The patient underwent percutaneous transluminal angioplasty (PTCA) of the proximal right coronary artery (RCA) and the proximal left coronary artery (LAD), whereas a 60%-lesion in the distal RCA was left untreated. **a** Anterior view (volume rendering mode) of thorax with ventral thorax wall cut away depicts situs inversus. **b** Right anterior oblique (RAO) projection of the circumflex artery (RCX) and prominent marginal branch in volume rendering mode. No high-grade lesion can be readily appreciated. **c** Maximum intensity projection (MIP) of RCX clearly shows a lesion (*arrow*). The degree of stenosis is estimated at 70%. **d** RAO cranial view of proximal LAD in volume rendering mode. The high-grade lesion was not clearly delineated in this view. **e** MIP image clearly depicted the lesion of the proximal LAD (*arrow*). **f** MIP of RCA in left posterior oblique projection. The *white arrow* depicts the distal RCA lesion. The *black arrow* shows the area of the former dilatation. No restenosis is present. **g** LAO cranial view of LAD and RCX with conventional angiography. The *arrows* depict the lesions in each of the vessels. **h** RAO view of RCA by conventional angiography. Note the progress of the former 60% lesion to a high-grade lesion (*arrow*) and the absent restenosis of the proximal RCA

Plaque imaging

It is widely accepted that only one-third of myocardial infarctions directly arise from significant coronary stenosis. Non-stenotic (<75%) plaques cause about 80% of deadly myocardial infarctions. Approximately 90% of all patients with acute myocardial infarction had no hemodynamically relevant lesion. Much more frequently, rupture of a vulnerable plaque with subsequent thrombus formation is the reason for occlusion of a coronary artery [27]. Most of the standard imaging techniques, however, identify only luminal diameter and stenosis; none can characterize plaque composition. Preliminary data indicate that MDCTA allows detection and assessment of noncalcified lipid-rich plaques (Fig. 3) [26, 28]. Schröder et al. [28] investigated noninvasive detection of coronary plaques and plaque composition by MDCT in comparison with intracoronary ultrasound (ICUS) as a gold standard. MDCT and ICUS yielded identical results regarding plaque composition and quantification of lesions [29]. Nikolaou et al. [40] also investigated the criteria that allow for morphological characterization of atherosclerotic coronary lesions based on MDCT imaging in human cadaver heart specimens. They compared the MDCT findings with histopathology, and found a high sensitivity for detection of types

Fig. 3. Noncalcified soft lipid-rich plaque in left anterior descending (LAD) coronary artery (*arrow*). Imaging was performed on a Somatom Sensation 4, with 120 cc Iomeprol 400. The plaque was confirmed at intracoronary ultrasound

IV, Va, Vb, and Vc atherosclerotic lesions according to the American Heart Association (AHA) classification [30]. Based on mean CT-attenuation, they reliably differentiated predominantly lipid-rich plaques from predominantly fibrous-rich plaques. Thus, this new technology holds promise for the noninvasive detection of rupture-prone soft coronary lesions and may lead to early onset of therapy [28, 31].

Function

With ECG-gated MDCT spiral scanning, two and three-dimensional images can be reconstructed in incrementally shifted heart phases with a temporal resolution of up to 125 ms. With multiplanar reformation, the heart can be displayed in any desired plane, such as the short and long axes. This allows functional analysis in a "one-stop shopping" approach for every patient undergoing CTA of the coronary arteries. The ability to obtain functional information from routine contrast-enhanced cardiac examinations on a conventional whole-body CT scanner could obviate the need for an additional study with a second imaging modality. Halliburton et al. [32] evaluated MDCT as a method for volume determination of the left ventricle by comparison to the gold standard, cine magnetic resonance imaging, in 15 patients with chronic ischemic heart disease. Left ventricular volume during end-diastole and end-systole volume measured with MDCT were significantly less than those measured with magnetic resonance imaging (MRI) on a fast gradient system. However, values for ejection fraction with MDCT and MRI were not statistically different. Similar results were reported by other authors [33, 34]. The exact determination of left ventricular volume during end-systole seems to be the most critical issue with a temporal resolution of ≥125 ms. Further improvement in temporal resolution will facilitate functional analysis.

When multiple cardiac phases are extracted, animated movies of the beating heart can be available. However, only limited data is available for the usefulness of the functional assessment of wall motion using MDCT. Mochizuki et al. [35] evaluated post-processing interactive multiplanar animation of wall motion in 15 patients in comparison with conventional left ventriculography [36]. By extracting multiple cardiac phases, interactive animated movies were generated. Extracted cardiac phases ranged from 8 to 11, depending on the patient's heart rate. The interactive animated movies were displayed in 6 planes and the left ventricle was divided into 7 segments according to the AHA classification. Wall motion was visually scored into 3 grades: normal, hypokinesis, and akinesis (severe hypokinesis to dyskinesis). The scores of MDCT and biplanar ventriculography agreed in 99 (94%) of 105 segments [35].

Myocardial perfusion

Myocardial perfusion defects are often observed as zones of low density in the risk area of acute myocardial infarction on contrast-enhanced helical CT [36]. However, the clinical meaning of this perfusion defect has not been elucidated. Koyama et al. [37] presented preliminary data on the potential role of CT in 45 patients with acute myocardial infarction in regard to the clinical outcome after successful reperfusion therapy. They visually assessed myocardial perfusion with respect to the depth of the perfusion defect. When compared with SPECT data, these data corresponded nicely to the non-viable infarct area; its depth allowed prediction of the outcome in the chronic phase. Even the volume of the infarcted area could be reliably assessed. In addition to these early perfusion defects, Koyama et al. [38] found that in some patients the perfusion defects disappeared when the CT scan was repeated several minutes later (late enhancement). Regarding the existence of early perfusion effect and late enhancement, they classified patients with acute myocardial infarction into 3 groups: group 1 showed no perfusion abnormalities, group 2 showed early perfusion defect and late enhancement, and group 3 showed persistent perfusion defect in early and late phases. Koyama et al. [38] concluded that this myocardial perfusion pattern on contrast-enhanced CT may predict clinical outcome of acute myocardial infarction after reperfusion therapy.

Assessment of more than one or two time points of enhancement and the calculation of classic myocardial perfusion parameters with MDCT are even more challenging. In a first attempt, Wintersberger et al. [39] analyzed myocardial contrast dynamics using ECG-triggered MDCT in 9 patients. A prospectively ECG-triggered transaxial dynamic scan (4×5 mm) over 35 heart beats was applied to analyze myocardial enhancement patterns with subsequent assessment of perfusion parameters. Quantitative flow calculations revealed values close to those within normal myocardium (0.73±0.20 ml/g min). In regions of impaired blood supply, amplitudes and upslopes of myocardial enhancement tended to be lower. They concluded that assessment of myocardial contrast dynamics is possible using MDCT, however, ventricular coverage and injection protocols need to be improved [39].

Limitations

With 4-row technology, a number of factors are known to decrease image quality of MDCTA and make image interpretation difficult [41]. The two factors mostly held responsible are higher heart rates and severe calcifications. Becker was one of the first to describe the negative effect of higher heart rates on image quality

[7]. These data have been confirmed by others [42]: excellent diagnostic image quality can only be obtained at heart rates < 65 bpm. The reason for this heart rate limitation lies in the temporal resolution of the CT image acquisition and reconstruction system. To obtain heart rates below 65 bpm for optimal image quality, either 80 mg esmolol intravenously or 50-100 mg metoprololtartrate orally can be administered prior to the scan.

Assessment of luminal diameter in the presence of severe calcifications yields unsatisfactory results. Especially if non-high grade coronary lesions are known, it can be difficult to determine the progress of that specific lesion. However there is only limited published data available that quantifies the amount of calcification critical for image interpretation. In a recent MDCTA study, we included a total of 66 patients with a history of coronary artery disease. Total calcium score as well as all coronary arteries including distal segments and side branches were assessed with respect to evaluability and the presence of coronary artery lesions or occlusions. Results were then compared to those from quantitative coronary angiography. Of all patients, only 24 (36%) were diagnosed correctly. In the other 42 patients, the clinical diagnosis was either not possible or incorrect. Artifacts due to elevated heart rates or severe coronary artery calcification were the main causes of degraded image quality inhibiting correct diagnosis. Analysis of the data suggested a threshold for maximum heart rate and maximum calcification (63 bpm and Agatston score 300, respectively). A second analysis was made using these thresholds. Now 22 (91%) of 24 patients were correctly diagnosed. This indicates that MDCTA can also be performed in patients with manifest coronary artery disease when selected properly within certain thresholds. Reasonable thresholds might be heart rate >63 bmp and severe calcifications with a total Agatston score >300.

From 4 to 16 rows

True isotropic resolution has not yet been reached with 4-slice CT systems. An increased number of simultaneously acquired slices and sub-millimeter collimation for cardiac applications will be the next steps on the way towards true isotropic scanning with multislice CT. The recently introduced multislice CT scanner Siemens SOMATOM Sensation 16, offering simultaneous acquisition of 16 slices with 0.75 mm or 1.5 mm collimated slice width each, is the first scanner of this new generation [43]. Similar to the 4-slice CT scanner SOMATOM Volume Zoom, the SOMATOM Sensation 16 has an adaptive array detector (Fig. 4). It consists of 24 detector rows: the 16 central ones are 0.75 mm wide in the center of rotation and the 4 outer ones on both sides are 1.5 mm wide. The total z-coverage in the iso-center is 24 mm. For calcium scoring, we use a collimation of 1.5 mm, while for CTA of the coronary arteries we use a collimation of 0.75 mm (13.2 mm/s feed) with a gantry rotation time of 420 ms. Spiral scanning with 16 sub-millimeter slices provides true isotropic resolution. As a consequence, the distinction between longitudinal and in-plane resolution will gradually become a historical remnant, and the traditional axial slice will loose its clinical predominance. In our first experience the new 16-slice computed tomography technique allowed accurate visualization of the entire coronary tree including the distal and side branches without respiratory and reconstruction artifacts (Figs. 5, 6).

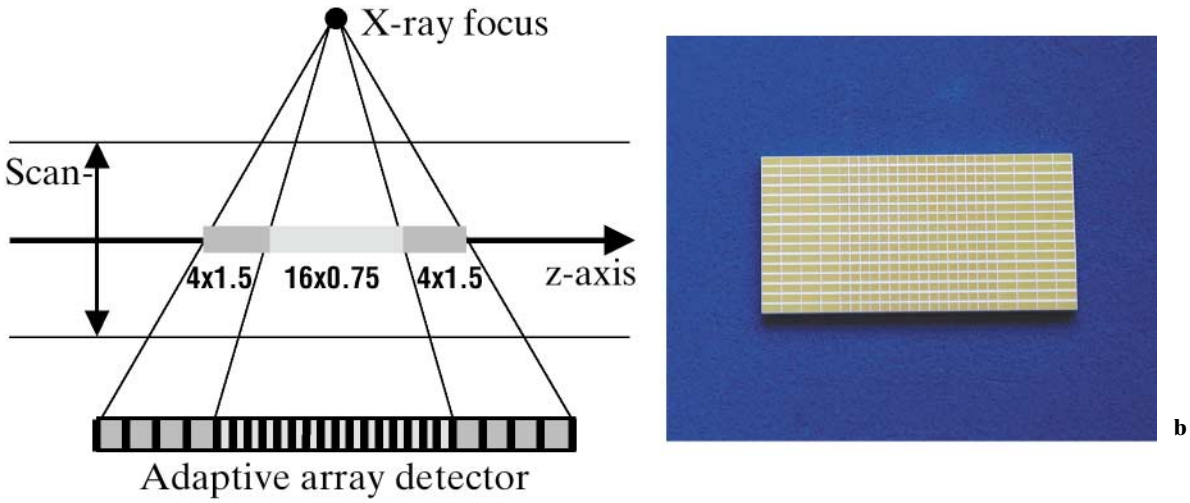

Fig. 4a, b. *Adaptive array detector used in the Siemens Somatom Sensation 16.* **a** By proper combination of the signals of the 24 detector rows, the basic collimations 16×0.75 mm and 16×1.5 mm can be realized. **b** Picture of a detector module, which consists of 16×24 detector elements

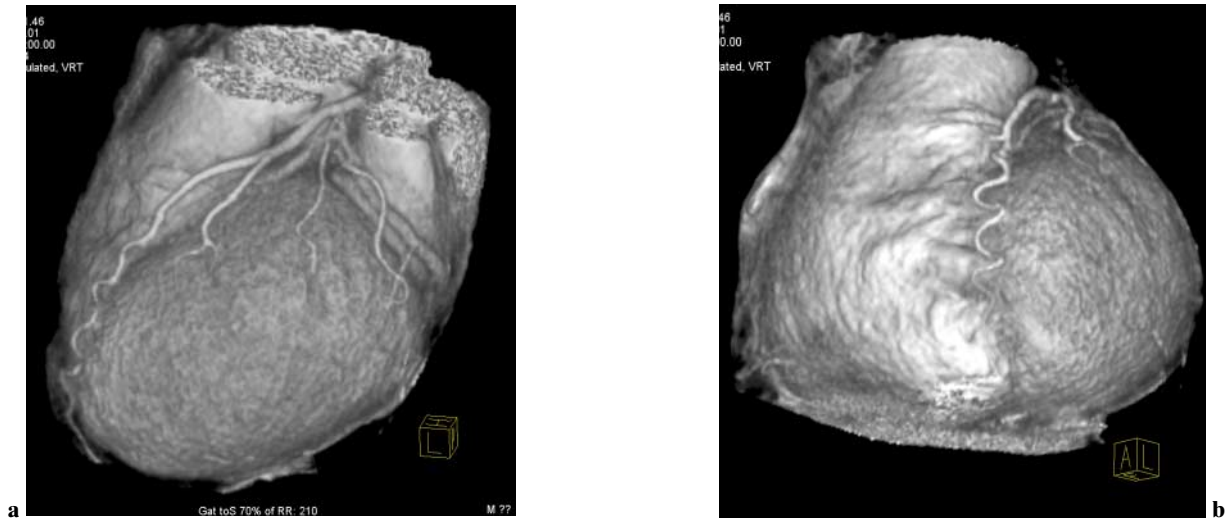

a b

Fig. 5 a, b. Coronary MDCT angiography with a 16-row CT-scanner (Somatom Sensation 16, 120 cc Iomeprol 400) in a 55-year-old woman presenting with atypical chest pain. CTA ruled out significant stenosis.

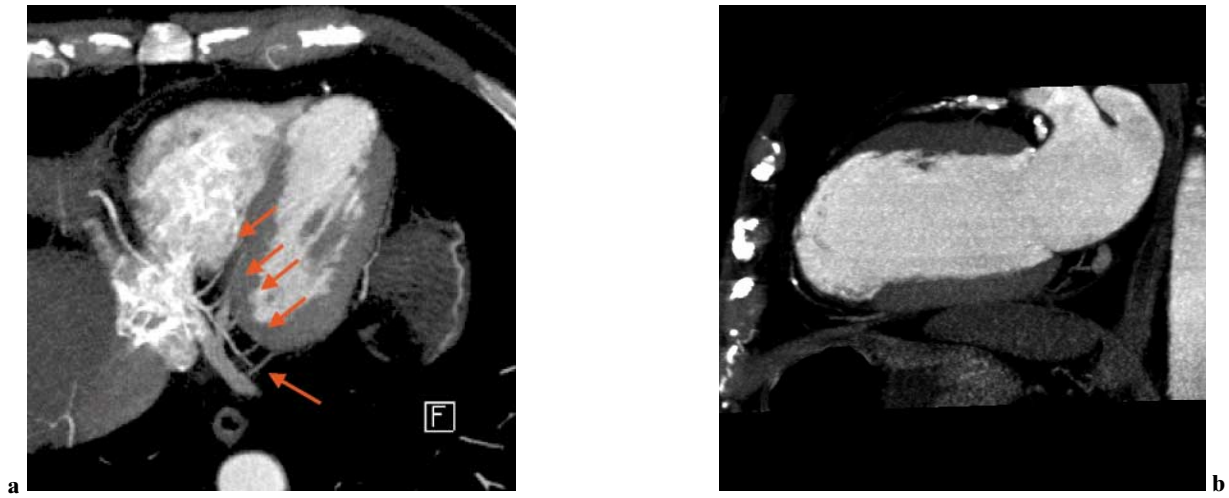

a b

Fig. 6 a, b. *A 66-year-old male patient with known single vessel coronary artery disease.* **a** MDCT angiography of the right coronary artery with a 16-row CT-scanner (Somatom Sensation 16, 120 cc Iomeprol 400). Even subsegmental branches (*arrows*) can be readily delineated. **b** Multiplanar Reformation (MPR) in the long axis depicts aneurysm of left ventricle status post myocardial infarction

X-ray exposure

Despite its undisputed clinical benefits, multislice scanning is often considered as increasing the radiation dose [44]. Indeed, a certain dose increase compared to single-slice CT is unavoidable due to the physical principles of multislice CT [45]. During ECG-gated spiral imaging of the heart, data are acquired with overlapping spiral pitch and continuous X-ray exposure. Thus, ECG-gated spiral acquisition requires higher doses than ECG-triggered sequential acquisition for a comparable signal-to-noise ratio. When performing multiple reconstructions in different cardiac phases for optimal image quality of individual vessels, all spiral data are used for image reconstructions and no data are omitted. To obtain the same diagnostic information, multiple sequential acquisitions would have to be performed with repeated injections of contrast material. This would eventually result in the same or even higher X-ray exposure. However, ECG-gated spiral acquisition by prospectively ECG-controlled online modulation of the tube output allows reduction of X-ray exposure [46]. By reduction of the tube output during heart phases that are not likely to be targeted by the ECG-gated reconstruction, dose savings up to 50% are possible. Dose is further reduced with increased number of simultaneously acquired slices. The collimated dose profile is in general a trapezoid in the axial direction. In the plateau region of the trapezoid, the entire focal spot is seen by the detector. In the penumbra regions, the focal spot is seen by the detector only partially, due to the limitation of the X-ray beam by the pre-patient collimator. With single-slice CT, the entire trapezoidal dose profile can contribute to the de-

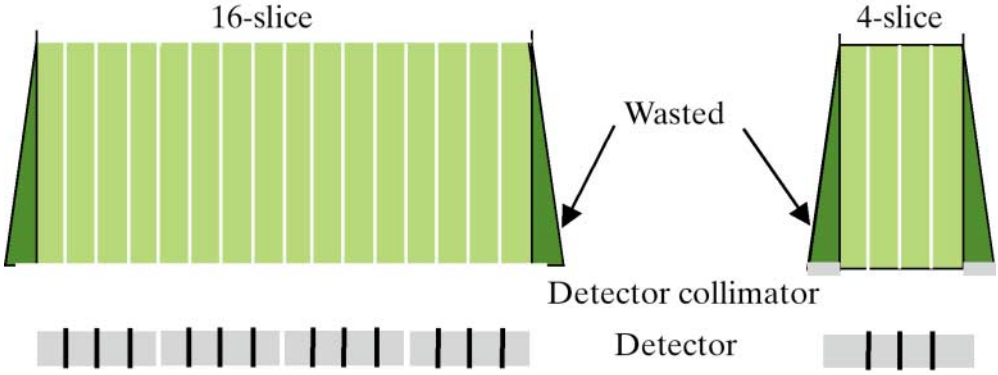

Fig. 7. Minimum width dose profiles for a 16-slice CT system and a corresponding 4-slice CT system with equal collimated width of one detector slice. The relative contribution of the penumbra region, which represents wasted dose, decreases with increasing number of simultaneously acquired slices

tector signal. With multislice CT, only the plateau region of the dose profile may be used to ensure equal signal level for all detector slices. The penumbra region has to be discarded, either by a post-patient collimator or by the intrinsic self-collimation of the multislice detector, and represents "wasted" dose. The relative contribution of the penumbra region increases with decreasing slice width, but it decreases with increasing number of simultaneously acquired slices. This is demonstrated in Fig. 7, which compares the "minimum width" dose profiles for a 4-slice CT system and a corresponding 16-slice CT system with equal collimated width of one detector slice. Correspondingly, the relative dose utilization of the 4-slice CT scanner SOMATOM Volume Zoom is 70% for 4×1 mm collimation and 85% for 4×2.5 mm collimation. The 16-row scanner has an improved dose utilization of 76%-82% for 16×0.75 mm collimation and 85%-89% for 16×1.5 mm collimation, depending on the size of the focal spot (large or small).

Conclusions

The emergence of multidetector-row CT has had significant impact on cardiac imaging. Cardiac calcium scoring and CTA of the coronary arteries as well as functional analysis are no longer limited to dedicated electron beam CT scanners. Cardiac imaging can now be performed on a standard body MDCT scanner. Even with 4-row technology, noninvasive MDCTA showed high diagnostic accuracy in the detection and quantification of coronary stenoses. In addition, this new technology holds promise to allow for the noninvasive detection and characterization of coronary atherosclerotic plaques.

References

1. Mannebach H, Hamm C, Horstkotte D (2001) 17th report of performance statistics of heart catheterization laboratories in Germany. Results of a combined survey by the Committee of Clinical Cardiology and the Interventional Cardiology (for ESC) and Angiology Working Groups of the German Society of Cardiology-Cardiovascular Research for the year 2000. Z Kardiol 90:665-667
2. Kwok BW, Lim TT (2000) Cortical blindness following coronary angiography. Singapore Med J 41:604-605
3. Kopp AF, Ohnesorge B, Flohr T et al. (2000) Multidetektor CT des Herzens: Erste klinische Anwendung einer retrospektiv EKG-gesteuerten Spirale mit optimierter zeitlicher und örtlicher Auflösung zur Darstellung der Herzkranzgefäße. Fortschr Röntgenstr 172:1-7
4. Sablayrolles JL, Besse F, Giat P (2001) Technical developments in cardiac CT: 2000 update. Rays 26:3-13
5. Gerber TC, Kuzo RS, Karstaedt N et al (2002) Current results and new developments of coronary angiography with use of contrast-enhanced computed tomography of the heart. Mayo Clin Proc 77:55-71
6. Janowitz WR (2001) Current status of mechanical computed tomography in cardiac imaging. Am J Cardiol 88: 35E-38E
7. Becker CR, Ohnesorge BM, Schoepf UJ et al (2000) Current development of cardiac imaging with multidetector-row CT. Eur J Radiol 36:97-103
8. Knez A, Becker C, Ohnesorge B et al (2000) Noninvasive detection of coronary artery stenosis by multislice helical computed tomography. Circulation 101:E221-E222
9. de Feyter PJ, Nieman K (2002) New coronary imaging techniques: what to expect? Heart 87:195-197
10. Nieman K, Oudkerk M, Rensing BJ et al (2001) Coronary angiography with multi-slice computed tomography. Lancet 357:599-603
11. Ohnesorge B, Flohr T, Kopp AF et al (2000) Cardiac imaging by means of electrocardiographically gated multisection spiral CT: initial experience. Radiology 217:564-571
12. Halliburton S, Chung K, Schvartzman P et al (2001) The use of ECG-referenced multi-slice Computed Tomography for the diagnosis of cardiovascular disease: comparison of sequential and spiral techniques. Radiology 221(P):412
13. Kopp AF, Schröder S, Küttner A et al (2001) Coronary arteries: retrospectively ECG-gated multi-detector row CT angiography with selective optimization of the image reconstruction window. Radiology 221:683-688
14. Becker CR, Knez A, Ohnesorge B et al (1999) Detection and quantification of coronary artery calcifications with prospectively ECG triggered multirow conventional CT and electron beam computed tomography: comparison of different methods for quantification of coronary artery calcifications. Radiology 213(P):351
15. Agatston A, Janowitz WR, Hildner FJ et al (1990) Quantification of coronary artery calcium using ultrafast computed

tomography. J Am Coll Cardiol 15:827-832
16. Ohnesorge B, Flohr T, Becker CR et al (1999) Comparison of EBCT and ECG-gated multislice spiral CT: a study of 3D Ca-scoring with phantom and patient data. Radiology 213(P):402
17. Carr JJ, Danitschek JA, Goff DC et al (2001) Coronary artery calcium quantification with retrospectively gated helical CT: protocols and techniques. Int J Card Imaging 17:213-220
18. Ohnesorge B, Knez A, Becker CR et al (2000) Reproducibility of coronary calcium scoring with EBCT and ECG-gated multi-slice spiral CT. Circulation 102:S405
19. Schoepf UJ, Becker CR, Obuchowski NA et al (2001) Multislice computed tomography as a screening tool for colon cancer, lung cancer and coronary artery disease. Eur Radiol 11:1975-1985
20. Haberl R, Steinbilger P (2001) New perspectives of non-invasive imaging with cardiac CT. J Clin Basic Cardiol 4:241-245
21. Kopp AF, Ohnesorge B, Flohr T et al (1999) Multidetector-row CT for the noninvasive detection of high-grade coronary artery stenoses and occlusions: first results. Radiology 213(P):435
22. Herzog C, Ay M, Engelmann K et al (2001) Visualisierungsmodalitäten in der Multidetektor CT-Koronarangiographie des Herzen: Korrelation von axialer, multiplanarer, dreidimensionaler und virtuell endoskopischer Bildgebung mit der invasiven Diagnostik. Fortschr Röntgenstr 173:341-359
23. Hong C, Becker CR, Huber A et al (2001) ECG-gated reconstructed multi-detector row CT coronary angiography: effect of varying trigger delay on image quality. Radiology 220:712-717
24. Georg C, Kopp AF, Schröder S et al (2001) Optimierung des Bild-Rekonstruktionszeitpunktes im RR-Intervall für die Darstellung der Koronararterien mittels Multidetektor-Computertomographie. Fortschr Röntgenstr 173:536-541
25. Knez A, Becker CR, Leber A et al (2001) Usefulness of multislice spiral computed tomography angiography for determination of coronary artery stenoses. Am J Cardiol 88:1191-1194
26. Schröder S, Kopp AF, Baumbach A et al (2001) Noninvasive detection and evaluation of atherosclerotic plaques with multislice computed tomography. J Am Coll Cardiol 37:1430-1435
27. Falk E, Fuster V (1995) Angina pectoris and disease progression. Circulation 92:2033-2035
28. Schröder S, Flohr T, Kopp AF et al (2001) Accuracy of density measurements within plaques located in artificial coronary arteries by multi-slice computed tomography: results of a phantom study. J Comput Assist Tomogr 25:900-906
29. Kopp AF, Ohnesorge B, Flohr T (1999) High temporal resolution ECG-gated multi-slice spiral CT: a new method for 3D and 4D cardiac imaging. Cardiovasc Intervent Radial 22:S184
30. Stary HC, Chandler AB, Dinsmore RE et al (1995) A definition of advanced types of atherosclerotic lesions and a histological classification of atherosclerosis. A report from the Committee on Vascular Lesions of the Council on Arteriosclerosis, American Heart Association. Circulation 92:1355-1374
31. Kopp AF, Schröder S, Baumbach A et al (2000) Non-invasive characterisation of coronary lesion morphology and composition by multislice computed tomography: first results in comparison with intracoronary ultrasound. Eur Radiol 11:1607-1611
32. Halliburton S, Petersilka M, Schvartzman P et al (2001) Validation of left ventricular volume and ejection fraction measurement with multi-slice computed tomography: comparison to cine magnetic resonance imaging. Radiology 221(P):452
33. Wintersperger BJ, Hundt W, Knez A et al (2002) Left ventricular systolic function assessed by ECG gated multirow-detector spiral computed tomography (MDCT): Comparison to ventriculography. Eur Radiol 12:S192
34. Juergens KU, Fischbach RM, Grude M et al (2002) Evaluation of left ventricular myocardial function by retrospectively ECG-gated multislice spiral CT in comparison to CINE magnetic resonance imaging. Eur Radiol 12:S191
35. Mochizuki T, Higashino H, Kayama Y et al (2001) Evaluation of wall motion using multi-detector-row CT: new application of post-processing interactive multi-planar animation of the heart. Radiology 221(P):413
36. Hilfiker PR, Weishaupt D, Marincek B (2001) Multislice spiral computed tomography of subacute myocardial infarction. Circulation 104:1083
37. Koyama Y, Matsuoka H, Higashino H et al (2001) Myocardial perfusion defect in acute myocardial infarction on enhanced helical CT after successful reperfusion therapy: a prognostic value. Radiology 221(P):195
38. Koyama Y, Matsuoka H, Higashino H et al (2001) Early myocardial perfusion defect and late enhancement on enhancement CT predict clinical outcome in patients with acute myocardial infarction after reperfusion therapy. Radiology 221(P):196
39. Wintersperger BJ, Ruff J, Becker CR et al (2002) Assessment of regional myocardial perfusion using multirow-detector computed tomography (MDCT). Eur Radiol 12:S294
40. Nikolaou K, Becker C, Barbaryka G et al (2001) High-resolution magnetic resonance and multislice CT imaging of coronary artery plaques in human ex vivo coronary arteries. Radiology 221(P):503
41. Kopp AF, Küttner A, Schröder S et al (2001) New developments in cardiac imaging: the role of MDCT. J Clin Basic Cardiol 4:253-260
42. Schroeder S, Kopp AF, Kuettner A et al (2002) Influence of heart rate on vessel visibility in noninvasive coronary angiography using new multislice computed tomography. Experience in 94 patients. Clin Imaging 26:106-111
43. Flohr T, Bruder H, Becker CR et al (2002) Isotropic submillimeter volume scannning of the heart with ECG-gated multislice spiral CT: first experience. Eur Radiol 12:S217
44. Cohnen M, Poll L, Puttmann C et al (2001) Radiation exposure in multi-slice CT of the heart. Fortschr Röntgenstr 173:295-299
45. Becker CR, Schatzl M, Feist H et al (1998) Strahlenexposition bei der CT-Untersuchung des Thorax und Abdomens. Vergleich von Einzelschicht-, Spiral- und Elektronenstrahlcomputertomographie. Radiologe 38:726-729
46. Ohnesorge B, Flohr T, Becker C et al (2000) Dose evaluation and dose reduction strategies for ECG-gated multi-slice spiral CT of the heart. Radiology 217(P):487
47. Kopp AF, Schröder S, Küttner A et al (2000) Multidetector-row CT for noninvasive coronary angiography: results in 102 patients. Radiology 217(P):375
48. Achenbach S, Giesler T, Ropers D et al (2001) Detection of coronary artery stenoses by contrast-enhanced, retrospectively electrocardiographically gated, multislice spiral computed tomography. Circulation 103:2535-2538
49. Nitatori T, Takahasi S, Yokoyama K et al (2001) Comparison of the detectability of coronary arterial stenotic lesions by MR angiography and multidetector CT. Radiology 221(P):200
50. Fischbach RM, Wichter T, Juergens KU. et al (2001) Mehrschicht-Spiral-CT (MSCT) der Koronararterien: Vergleich mit der Koronarangiographie. Fortschr Röntgenstr 173:S26
51. Herzog C, Diebold T, Dogan S et al (2001) Value and limits of multislice-cardiac-CT: a prospective study in over 500 patients. Radiology 221(P):412